THE ASTROPHYSICAL JOURNAL, 505:376–389, 1998 September 20
© 1998. The American Astronomical Society. All rights reserved. Printed in U.S.A.

CURRENT SHEETS AND PROMINENCE FORMATION IN THE SOLAR ATMOSPHERE

C. Z. CHENG AND G. S. CHOE[1]
Princeton Plasma Physics Laboratory, Princeton University, P.O. Box 451, Princeton, NJ 08543-0451
Received 1997 November 6; accepted 1998 April 21

ABSTRACT

If magnetic field lines in opposite directions expand toward each other to squeeze out the field between them, they come into contact to form an abrupt field reversal (tangential discontinuity) which supports a current sheet. Field line expansion can be caused by the combined pressure gradient and gravity force, the magnetic field pressure gradient force, magnetic fields merging toward each other, or a combination of these effects. In this paper we show that in a quadrupolar magnetic field geometry magnetohydrostatic (MHS) equilibria without null point can be deformed into equilibrium field configurations containing current sheets by changes in forces associated with thermodynamic properties or field line footpoint displacement. The shape of current sheets depends on the pressure distributions and footpoint displacement profiles. These MHS equilibria containing current sheets can evolve into different prominence magnetic field configurations via resistive magnetic reconnection processes to support a higher plasma density at the reconnection site than its surrounding. Examples are given to demonstrate these physical processes. If the plasma pressure (or density) on the photospheric boundary is higher in the lower flux tubes than in the higher tubes in each bipolar arcade, the combined pressure gradient and gravity force pushes magnetic field lines outward from the center of each bipolar arcade. When the plasma temperature increases above a critical value, the enhanced expansion of these arcade fields results in the formation of a current sheet between these two arcades along a separatrix line. Similarly, if the field line footpoints undergo a spatially continuous shearing motion so that the outward gradient force of the sheared magnetic field pressure pushes the field lines of each bipolar arcade into contact, a current sheet of the same shape is formed when the amount of shear is above a critical value. This field configuration can be deformed into a configuration with an X-point through resistive magnetic reconnection. It is expected that an inverse polarity prominence can stably reside above the X-point. If the plasma pressure (or density) on the photospheric boundary is lower in the lower flux tubes than in the higher tubes in each bipolar arcade, the combined pressure gradient and gravity force which pushes down magnetic field lines is reduced when the atmosphere is cooled. When the temperature is decreased below a critical value, the subsequent expansion of field lines due to the magnetic tension force creates a new current sheet configuration with a sharp downward-pointing tip hanging at a distance above the bottom boundary. Resistive magnetic reconnection in this type of current sheet results in a Malville-type field configuration with a magnetic island wrapped in dipped field lines. It is expected that an inverse polarity prominence can stably reside within the magnetic island. Our results suggest that the formation of MHS equilibria containing current sheets and their evolution into prominence magnetic field configurations must be a general process in the solar atmosphere.

Subject headings: numerical — MHD — Sun: prominences — Sun: magnetic fields

1. INTRODUCTION

It is widely believed that solar eruptive phenomena and coronal heating involve fast magnetic reconnection processes which convert coronal magnetic energy into kinetic and thermal energies. It is also often speculated that the magnetic field around a solar prominence has a helical structure, which results from reconnection of sheared magnetic field in a current sheet (e.g., Kuperus & Raadu 1974). Because the plasma is rather collisionless in the solar corona with the magnetic Reynolds number on the order of 10^{12}–10^{14}, resistive magnetic reconnection is expected to occur only if a very thin current sheet exists with width on the order of an ion gyroradius (~ 10 m in typical corona). It is thus important to understand how such a thin current sheet is formed.

Current sheets can be related to solar prominence in two aspects. First, the slablike appearance and the high mass density of prominence require highly bent field lines in the prominence vicinity. This is a morphological aspect. There have been a series of studies along this line, in which magnetohydrostatic (MHS) equilibrium solutions with a massive current sheet are sought as an approximation of prominence-embedding magnetic fields (e.g., Aly & Amari 1989; Lepeltier & Aly 1996). In these studies, however, the presence of current sheets is assumed a priori and their origin has not been addressed. The second aspect regards the formation of solar prominence. Solar prominences are often observed between the opposing fields of two active regions (Martin 1973; Tang 1987), and the cancellation of magnetic patches of opposite polarities is regarded as one of the observational conditions in prominence-forming regions (Martin 1990). This suggests that solar prominences are often formed in a current sheet and the evolution of current sheet due to magnetic reconnection can lead to the prominence formation.

Except during a dynamical phase related to some instabilities or magnetic reconnection processes, the solar plasma is in a quasi-equilibrium state because the wave

[1] Presently at Tongmyong University of Information Technology, Pusan 608-080, Korea.

transit time along magnetic field lines is generally much shorter than the timescale of boundary motions or global change of thermodynamic properties. During this quasi-static evolution, the ideal MHD condition is valid due to the large magnetic Reynolds number of the system. The quasi-static evolution of solar plasma can be approximated by a sequence of equilibria determined by continuously changing physical parameters. When the physical parameters change continuously in space and in time, the sequence of corresponding equilibrium states may be expected to have continuity.

Parker (1972) first proposed that infinitely thin current sheets tend to be formed in a perfectly conducting magnetoplasma when the endpoints of field lines are arbitrarily moved. Across the current sheet the magnetic field is allowed to be discontinuous, but the total pressure (sum of magnetic and plasma pressures) must be continuous. The MHS equilibrium containing a current sheet is usually called a *weak equilibrium.* In a series of studies (Parker 1994, and references therein), Parker showed that the formation of current sheets are unavoidable in MHS equilibria under the constraint of a fixed field topology, and he called this property "the fundamental theorem of magnetohydrostatics." Although this argument at times led to controversies (e.g., van Ballegooijen 1985, 1988), some studies indicated that spontaneous formation of current sheets is inevitable (Low 1987; Low & Wolfson 1988). While most studies along this line are concerned with field line footpoint motions, Low (1992) demonstrated an example of current sheet formation by pressure profile variation.

In this study, we are particularly interested in the continuity of magnetic field line connectivity or field topology. However, it is often the case that the topological continuity of the equilibrium sequence breaks down, and this happens if, beyond a critical value of a system parameter, no equilibrium can be found in the initial field topology, but an equilibrium exists in a different field topology. This nonexistence of solutions in a certain topology is called *global singular nonequilibrium* (GSNE) (Aly 1994). However, the transition to a different topology can be caused only by magnetic reconnection, which is not allowed as long as the ideal MHD condition is valid. Thus, instead of a topological transition, some oppositely directed field lines collapse to form a current sheet, i.e., a tangential discontinuity. Of course, the weak equilibrium state can be converted to a smooth equilibrium in a different topology by the magnetic reconnection process. In this aspect, a weak equilibrium state may be considered as a metastable state. In a system with a very large magnetic Reynolds number, such a metastable state would necessarily appear before the magnetic reconnection process via some resistive instabilities is initiated.

The current sheet in a weak equilibrium is different from an asymptotically thinning current layer in a sequence of smooth equilibria, such as the current layer developed in a sheared bipolar arcade (e.g., Mikić & Linker 1994; Choe & Lee 1996a). This current layer becomes infinitely thin asymptotically as the footpoint displacement increases indefinitely. Thus, a smooth equilibrium containing such a current layer can exist for any finite amount of footpoint displacement. The simulation studies by Mikić & Linker (1994) and Choe & Lee (1996b) show the possibility of magnetic reconnection in such current layers with a small magnetic Reynolds number on the order of 10^5. However, with a more realistic magnetic Reynolds number of 10^{12} the magnetic reconnection may be too slow to be of relevance because there may be no resistive instability and magnetic field reconnection can occur only via a very slow resistive diffusion process.

In this paper we present the formation of two-dimensional MHS equilibria with thin current sheets (Cheng & Choe 1997) in a quadrupolar magnetic field geometry. We also demonstrate numerically the evolution of these two-dimensional thin current sheet equilibria into prominence-like structures via resistive magnetic reconnection. Our study is focused on tangential discontinuities generated by GSNE. Because GSNE does not seem to occur in a single bipolar arcade, we consider quadrupolar fields generated by two positive and two negative poles. Such a combination of polarities is thought to be quite ubiquitous in the solar surface, especially in flaring regions and prominence-forming regions. Recent observation by the soft X-ray telescope (SXT) aboard *Yohkoh* satellite revealed the quadrupolar field geometry of the coronal structure surrounding high latitude dark filaments (Uchida et al. 1997a). We expect that any possible mechanism of current sheet formation in the quadrupolar field geometry would work in the real solar magnetic fields, which usually exhibit more complex geometries.

It is well known that a field configuration with a null-point or null-line tends to be deformed into a current sheet configuration by a small disturbance (Syrovatskii 1981; Uchida et al. 1997b), so we will not consider such cases, but rather consider field configurations without any null-point. To obtain weak equilibrium solutions with thin current sheets, we consider two different types of change in the solar environment: change of the thermodynamic properties, such as temperature or entropy, of the whole atmosphere and continuous motion of field line footpoints at the boundary. We found that critical values of control parameters exist for which the equilibrium magnetic field changes from a smooth function of space to one with a tangential discontinuity. In such thin current sheet configurations, magnetic reconnection can be triggered by plasma collisional or anomalous resistivity.

The current sheet formation by effects of plasma pressure gradient force and field line footpoint displacement that we are going to demonstrate in this paper can be understood in the following intuitive terms. In a two-dimensional isothermal plasma under a uniform gravity pointing downward in the z-direction, the plasma pressure and mass density can be written as $[P(A, z), \rho(A, z)] = [\hat{p}(A), \hat{\rho}(A)]e^{-z/H}$, where A is the magnetic flux function and H is the scale height related to the plasma temperature and gravitational constant. The combined pressure gradient and gravitational force is in the $-\nabla\hat{p}(A)$ direction. Depending on the distribution of $\hat{p}(A)$, different current sheet configurations can result from changes in the plasma temperature. If $\hat{p}(A)$ is higher in the inner flux tubes than in the outer tubes, the combined pressure and gravity force pushes plasma and magnetic field outward to balance the magnetic field line tension force. When the plasma temperature increases above a critical value, the enhanced pressure gradient force pushes out the field lines in each bipolar region so that a thin current sheet of a finite length forms at the region where the field lines from each bipolar region come into contact. The current sheet in this case grows in height from the bottom boundary. If resistivity is applied to this current sheet configu-

ration magnetic reconnection changes the field topology into one with an X-point. Such a transition may be involved in certain types of solar flares.

If $\hat{p}(A)$ is higher in the outer magnetic flux tubes than in the inner tubes, temperature reduction in the atmosphere can lead to the formation of a different current sheet topology. As the combined pressure gradient and gravitational force, which pushes field lines downward, is reduced by the cooling of the atmosphere, the magnetic field tension force expands outward in the upper part of the flux tubes. The subsequent expansion of field lines creates a tangential discontinuity as the plasma temperature is below a critical value. A new current sheet configuration is formed with a sharp-pointed end of the current sheet hanging at a distance above the bottom boundary. If the plasma resistivity is considered in this weak equilibrium state, magnetic reconnection results in a Malville type field configuration with a magnetic island hanging in the solar atmosphere. It is expected that a prominence can stably reside within the magnetic island.

When the field line footpoints undergo a shearing motion with a continuous shearing profile, a current sheet can be formed beyond a critical amount of shear. This is an example of current sheet formation by general footpoint displacement by Parker (1972). This mechanism of current sheet formation is similar to the case with change in the plasma heat content because a field line footpoint shear is to produce a magnetic field in the footpoint shearing direction, and the resultant shear magnetic field pressure is equivalent to an increase in the plasma heat content. Depending on the shear magnetic field pressure as a function of the magnetic flux the shear magnetic field pressure gradient force can either expand or depress the field lines just like the combined pressure gradient and gravitational force. We have demonstrated that the footpoint shearing motion can produce the current sheet configurations as in the cases of temperature changes.

Our study clearly demonstrates that diverse mechanisms can lead to weak equilibria and suggests the the current sheet formation is a rather universal phenomenon in the solar atmosphere. In § 2, a general account is given for the two-dimensional MHS equilibrium problem, Low's analytical solutions (Low 1992) are briefly reviewed, and our problem setting is presented. In § 3, the current sheet formation by thermodynamic change (atmospheric heating and cooling) is presented. In § 4, we discuss the current sheet formation by field line footpoint shearing. In § 5, the relationship between current sheets and prominence formation is given. Finally, a brief summary and discussion is given in § 6.

2. TWO-DIMENSIONAL MHS EQUILIBRIUM PROBLEMS

Our studies of the equilibrium thin current sheet formation are based on an MHD model for isotropic pressure plasma under a gravitational force. The momentum equation in the rationalized EMU unit is given by

$$\rho \frac{d\boldsymbol{v}}{dt} = \boldsymbol{J} \times \boldsymbol{B} - \nabla P + \rho \boldsymbol{g} + \nabla \cdot \mu \nabla \boldsymbol{v} - \lambda \rho \boldsymbol{v} , \qquad (1)$$

where $(d/dt) = (\partial/\partial t) + \boldsymbol{v} \cdot \nabla$ is the total time derivative, $\boldsymbol{v}$ is the fluid velocity, $\boldsymbol{B}$ is the magnetic field, P is the plasma pressure, ρ is the total plasma mass density, $\rho \boldsymbol{g}$ is the gravitational force, μ is the plasma viscosity, and λ is the frictional force coefficient. The mass density continuity equation is given by

$$\frac{d}{dt} \rho + \rho \nabla \cdot \boldsymbol{v} = 0 . \qquad (2)$$

Maxwell's equations with the magnetostatic approximation hold: Faraday's law,

$$\frac{\partial \boldsymbol{B}}{\partial t} = -\nabla \times \boldsymbol{E} , \qquad (3)$$

where $\boldsymbol{E}$ is the electric field; Ampere's law,

$$\boldsymbol{J} = \nabla \times \boldsymbol{B} ; \qquad (4)$$

and Gauss law,

$$\nabla \cdot \boldsymbol{B} = 0 . \qquad (5)$$

To close the above equations, equations (1)–(5), we need to prescribe a relation between the electric field and the fluid velocity as well as the dynamics of plasma pressure. If plasma kinetic effects can be ignored, Ohm's law,

$$\boldsymbol{E} + \boldsymbol{v} \times \boldsymbol{B} = \eta \boldsymbol{J} , \qquad (6)$$

where η is the plasma resistivity, is usually employed so that the perpendicular fluid motion is mainly determined by the $\boldsymbol{E} \times \boldsymbol{B}$ motion. We assume, for simplicity, an ideal gas law so that the plasma pressure is related to the mass density by

$$P = R_0 \rho T , \qquad (7)$$

where R_0 is the gas constant and T is the plasma temperature which is usually not a constant in space. This ideal gas law is justified by a high thermal conductivity in the corona and is regarded to fit better in modeling the slow evolution of the corona than the common assumption of adiabaticity with the ratio of specific heat to be 5/3. These MHD equations will be solved to obtain equilibrium solutions by demanding that the fluid velocity be asymptotically small.

2.1. *Two-dimensional MHS Equilibrium Equations*

The quasi-static solar equilibrium with isotropic pressure under a uniform gravitational force satisfies

$$\boldsymbol{J} \times \boldsymbol{B} = \nabla P + \rho g \nabla z , \qquad (8)$$

where g is the gravitational constant and the gravitational force is pointing downwards in the z direction. If there is no field line reconnection, a magnetic field that is a function of x and z can be expressed by

$$\boldsymbol{B} = \boldsymbol{B_p} + B_y \nabla y , \qquad (9)$$

where $\boldsymbol{B_p} = \nabla A(x, z) \times \nabla y$ is the poloidal magnetic field, B_y is the toroidal magnetic field, the equilibrium quantities are independent of y, and the magnetic field lines lie in constant poloidal magnetic flux function $A(x, z)$ surfaces because $\boldsymbol{B} \cdot \nabla A(x, z) = 0$. Then, because $\boldsymbol{J} \times \boldsymbol{B} \cdot \nabla y = -\boldsymbol{J} \cdot \nabla A = 0$, we have $\boldsymbol{B} \cdot \nabla B_y = 0$. From $\boldsymbol{B} \cdot \nabla A = 0$, B_y must be a function of A only.

If we write the pressure in the form $P(x, z) = \hat{p}(A) f(x, z)$ and make use of the ideal gas law, then $f(x, z)$ is uniquely determined from $\boldsymbol{B} \cdot (\nabla P - \rho \boldsymbol{g}) = 0$ and is given by $f(x, z) = e^{-z/H(A)}$, where $H(A) = R_0 T(A)/g$ can be interpreted as a scale height. Then, the equilibrium plasma pressure and mass density have the formal solutions (Dungey

1953):

$$P(z, A) = \hat{p}(A)e^{-z/H} , \quad (10)$$

and

$$\rho(z, A) = \hat{\rho}(A)e^{-z/H} , \quad (11)$$

where $\hat{\rho}(A) = \hat{p}(A)/gH(A)$. If H is a constant, $\hat{\rho}(A)$ has the same spatial variation as $\hat{p}(A)$. Note that the plasma pressure and mass density are not constant along the field line. The pressure gradient and gravitational forces can be combined to be

$$-(\nabla P + \rho g \nabla z) = -\left[\nabla \hat{p}(A) + \frac{\hat{p}z}{H^2} \nabla H(A)\right] e^{-z/H} . \quad (12)$$

Note that the downward gravitational force is cancelled by a part of the pressure gradient force, and the combined force is in the $\pm \nabla A$ direction through $\nabla \hat{p}(A)$ and $\nabla H(A)$ terms. If H (or temperature) is a constant, then the combined force is in the $-\nabla \hat{p}(A)$ direction. Because the plasma is frozen in the field lines, the combined force is to expand the magnetic field lines outward toward the larger A region if $(d\hat{p}/dA) < 0$, and vice versa.

The $\boldsymbol{J} \times \boldsymbol{B}$ force can be decomposed into two components,

$$\boldsymbol{J} \times \boldsymbol{B} = (\nabla \times \boldsymbol{B_p}) \times \boldsymbol{B_p} - \nabla\left(\frac{B_y^2}{2}\right) . \quad (13)$$

The first term represents the $\boldsymbol{J} \times \boldsymbol{B}$ force due to $\boldsymbol{B_p}$ and contains the magnetic flux function $A(x, z)$ only, and the second term is the toroidal magnetic field pressure gradient force. Therefore, the toroidal magnetic field pressure gradient force has a similar effect as the combined pressure gradient and gravitational force in determining the magnetic flux function $A(x, z)$.

The toroidal current (in the y-direction) is given by

$$J_y(z, A) = \frac{d}{dA}\left(\frac{B_y^2}{2}\right) + \left(\frac{d\hat{p}}{dA} + \frac{\hat{p}z}{H^2}\frac{dH}{dA}\right)e^{-z/H} , \quad (14)$$

and the poloidal current (in the $\nabla A \times \nabla y$ direction) is given by

$$J_p(A) = \boldsymbol{J} \cdot \frac{\nabla A \times \nabla y}{|\nabla A|} = \nabla B_y \cdot \frac{\nabla A}{|\nabla A|} . \quad (15)$$

The magnetic flux function $A(x, z)$ satisfies the Grad-Shafranov equation,

$$\nabla^2 A(x, z) = -J_y(z, A) . \quad (16)$$

To solve the Grad-Shafranov equation we need to specify the functions $\hat{p}(A)$, $H(A)$, and $B_y(A)$ in addition to the boundary condition.

2.2. *Analytical Quadrupolar Field Solutions*

Analytical two-dimensional MHS solutions (Zweibel & Hundhausen 1982; Low 1992) have been obtained from the Grad-Shafranov equation, equation (16), by considering $B_y = 0$ and a uniform temperature (H is a constant), and a $\hat{p}(A)$ that is quadratic in A and is given by $\hat{p}(A) = aA^2 + \hat{p}_0$, where a is related to the pressure gradient scale. For $a > 0$, the general solution can be expressed as a linear superposition of the infinite set of separable solutions of the form (Zweibel & Hundhausen 1982),

$$A_k = J_s(qe^{-z/2H})e^{ikx} , \quad (17)$$

where k is the Fourier wave number associated with x and J_s is a Bessel function of order $s = \pm 2kH$ with $q^2 = 8aH^2$. For $a < 0$, J_s is replaced by the modified Bessel function I_s.

Because it is quite common in solar active regions to have four sun spots with different polarities one after another, we will consider quadrupolar field geometries that mimic such a combination of field polarities. The effect of plasma pressure on the formation of thin current sheet has been studied (Low 1992) by employing the quadratic profile of $\hat{p}(A)$ and by considering the following boundary conditions: $A = 0$ at $x = \pm\pi/2k$; $A \to 0$, as $z \to \infty$; and $A = B_0(\cos kx - a_3 \cos 3kx)/k$ at $z = 0$, where $1 > a_3 > 0$. From equation (14) $J_y = 0$ for $a = 0$, and a simple potential field solution is given by

$$A_0(x, z) = \frac{B_0}{k}\left[e^{-kz}\cos(kx) - a_3 e^{-3kz}\cos(3kx)\right] , \quad (18)$$

where B_0 is a normalized constant magnetic field intensity and a_3 is a constant. It should be noted that the field in the half-plane $z > 0$ can have an X-type neutral point depending on the parameter a_3, which represents the relative strength of the third harmonic to the first harmonic field. The field is bipolar for $a_3 \leq \frac{1}{9}$, quadrupolar without neutral points for $\frac{1}{9} < a_3 \leq \frac{1}{3}$, and quadrupolar with an X-type neutral point for $a_3 > \frac{1}{3}$. The value of a_3, above which an X-point appears in the equilibrium field for a given a, will be denoted by a_{3X}. For $a = 0$, $a_{3X} = \frac{1}{3}$.

For $a < 0$, the pressure is depressed in the lower arcades with the pressure becoming lower toward the center of the lower bipolar arcades, where A is maximum. The equilibrium solution is given by

$$A_-(x, z) = \frac{B_0}{k}\left[\frac{I_s(|q|e^{-z/2H})}{I_s(|q|)}\cos(kx) - a_3\frac{I_{3s}(|q|e^{-z/2H})}{I_{3s}(|q|)}\cos(3kx)\right] . \quad (19)$$

In comparison with the potential field solutions ($a = 0$), the magnetic field is everywhere compressed downward toward the $z = 0$ boundary by the negative pressure gradient and the gravity. Consequently, there can be no X-point in the equilibrium field configuration even for $a_3 > \frac{1}{3}$.

For $a > 0$, the pressure is increasing toward the center of the two lower bipolar arcades, and the equilibrium solution with a periodic quadrupolar field geometry is given by

$$A_+(x, z) = \frac{B_0}{k}\left[\frac{J_s(qe^{-z/2H})}{J_s(q)}\cos(kx) - a_3\frac{J_{3s}(qe^{-z/2H})}{J_{3s}(q)}\cos(3kx)\right] . \quad (20)$$

Because of the positive plasma pressure gradient ($a > 0$), the magnetic field line will expand outward toward lower flux region in order to confine the plasma. As the pressure gradient (or a) increases, the magnetic field lines keep expanding outward toward each other to compress the magnetic flux external to them. Thus, the equilibrium field configuration can have an X-point even for $a_3 < \frac{1}{3}$, i.e., a_{3X} becomes smaller as a become larger. Low (1992) deduced that as a increases over a critical value, say a_{crit}, the oppositely expanding magnetic field lines will come into

contact by expelling all the external flux. If there is no topological constraint, for a given a_3 the field will change from a configuration without X-point for a $< a_{\rm crit}$ to one with an X-point for $a > a_{\rm crit}$. However, if the ideal MHD constraint is valid, the topological transition is inhibited. Thus, from this property he reasoned that if a is slowly increased from below $a_{\rm crit}$ with a field topology without X-points to over $a_{\rm crit}$, the magnetic field will end up in a weak equilibrium state embedding a current sheet. Across the current sheet the magnetic pressure is continuous, but the tangential magnetic field reverses abruptly.

There are a few characteristic features of Low's current sheet, which were not discussed in his paper (Low 1992). As shown in the sketch in Figure 1, Low's current sheet is extended from the origin (O) to a point Q lying on the z-axis and along OQ, $J_y = -\infty$. The field line segment PQ lies in the same field line as the current sheet QO, but it does not form a current sheet because $d\hat{p}/dA$ is finite there. In MHS equilibria, the sum of plasma pressure must be continuous across any field line including a current sheet, i.e.,

$$\left[p + \frac{B^2}{2}\right] = 0 , \tag{21}$$

where the bracket denotes the difference of the value of the function in the bracket on each side of a surface containing the field line. Because Low's current sheet is obtained by imposing a continuous $\hat{p}(A)$ profile, the magnetic field must be continuous everywhere including across PQ and QO. If the field configuration in the neigborhood of Q is like a cusp, the field strength vanishes as Q is approached from above in domain Ω_3. However, if Q is approached in domain Ω_1 or Ω_2, the field strength does not vanish. Then, equation (21) cannot be satisfied. The only way to resolve this problem is for the field line segments PQ, QR, and QO to meet at Q with nonzero angles so that the field strength may become zero as Q is approached from all directions. Thus, Low's field configuration in the neighborhood of Q must be a Y-shape (Low & Wolfson 1988). The volume per unit flux, which will be called the differential flux volume, is given by

$$V(A) = \int_A \frac{dl}{B} , \tag{22}$$

where the integration is performed along the field line labeled by the flux function A. The differential flux volume generally becomes infinity for field lines connected to an X- or Y-point with only one known exception of a smooth field configuration containing an X-pont (Lau & Finn 1990). The entropy content per flux tube can be measured

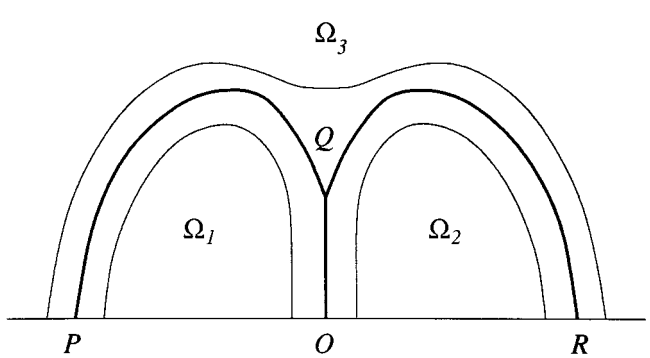

FIG. 1.—Sketch of the magnetic field line structure of a current sheet

by the function $S(A)$, which we call the differential entropy content, defined by

$$S(A) = \int_A \frac{p^{1/\gamma}}{B} dl , \tag{23}$$

where γ is the ratio of specific heats. In Low's current sheet, the pressure is nonzero and continuous everywhere and thus the differential entropy content is infinite. This, however, does not mean that an infinite amount of entropy is needed for the system, because the entropy content in a finite flux can be finite, i.e.,

$$\int_{A_c - \Delta A}^{A_c + \Delta A} S(A) dA < \infty , \tag{24}$$

where A_c is the flux function of the current sheet and $\Delta A > 0$. In low's model, the control parameter is the pressure gradient. To maintain a certain pressure profile, certain processes must selectively supply more entropy to those flux tubes where the current sheets form. However, the location of the current sheet is not known before the system settles down to an equilibrium. To overcome these difficulties, we will formulate the current sheet problem differently as described in the following.

2.3. *Problem Setting*

Instead of solving the Grad-Shafranov equation for $A(x, z)$ by prescribing the functions $\hat{p}(A)$ and $B_y(A)$ directly, we shall obtain $\hat{p}(A)$ and $B_y(A)$ by employing additional physical constraints. Physically, we can think of two ways of changing the plasma pressure in each flux tube. One is to supply (drain) mass to (from) the flux tube by photospheric evaporation or siphon processes, and the other is to heat or cool the plasma in the flux tube. Of course, a combination of both mechanisms is possible. In this paper we will consider the pressure change by a temperature change and the photosphere is considered to be quite rigid. If there is no magnetic reconnection and if the plasma cross field diffusion time is long in comparison with the typical timescale of thermal dynamical change and/or footpoint motion, the total mass per unit flux tube must be conserved in the domain above a rigid surface. Therefore, in addition to the topological constraint, we will impose the invariance of the mass per unit flux,

$$M(A) = \int_A \frac{\rho}{B} dl , \tag{25}$$

as another constraint and choose the temperature as the control parameter. With this setup, we actually impose the entropy content per flux tube not directly in the form of equation (23), but in a similar form given by

$$\tilde{S}(A) = \int_A \frac{P}{B} dl = R_0 T(A) M(A) , \tag{26}$$

which is equivalent to equation (23) when $\gamma = 1$. To simplify the problem, we further assume that the temperature is constant everywhere. Thus, the functional form of $\tilde{S}(A)$ is set by $M(A)$, its magnitude is determined additionally by T, and the entropy content per unit flux tube never diverges. By choosing a $M(A)$ profile, $\hat{p}(A)$ is uniquely determined if other thermodynamic properties are fixed. However, as thermodynamic properties such as the plasma temperature are varied, the equilibrium magnetic field will change and, therefore, a new $\hat{p}(A)$ will be obtained. This procedure is

rather nonlinear and can be achieved only through numerical calculations.

The $B_y(A)$ can be obtained by introducing either the field line footpoint shearing motion in the y-direction or the field-aligned current. If the field line footpoints of a magnetic field configuration without the toroidal magnetic field are displaced in the y direction, a magnetic field in the y-direction will be produced. The distance in the y-direction between two footpoints of a field line is given by

$$\zeta(A) = \int_A \frac{B_y}{B}\, dl = B_y(A)V(A)\,, \tag{27}$$

which is the B_y flux per tube. From equations (14) and (16) we see that the gradient of B_y^2 plays a similar role as the gradient of $\hat{p}$ in determining the equilibrium configuration. Comparison between this equation and equation (23) shows that $\zeta(A)$ is equivalent to $S(A)$ when $\gamma = 2$. This is quite natural because the magnetic pressure gradient force is in the direction perpendicular to the magnetic field direction. As in the case of imposing a continuous profile of $\hat{p}(A)$, a continuous profile $B_y(A)$ may be able to create a current sheet in the equilibrium solution. Then, the footpoint distance $\zeta(A)$ diverges at the separatrix just as $S(A)$ diverges in the other case. An infinite amount of footpoint distance cannot be realized. Thus, we will deal with the problem in which the footpoint displacement is given as the control parameter. We now define the total footpoint displacement for flux function A as

$$\zeta(A) = \sum_i \int_{A_i = A} \frac{B_{yi}}{B_i}\, dl = \sum_i B_{yi}(A)V_i(A)\,, \tag{28}$$

where the subscript i denotes the different field lines for the same A. As mentioned earlier, the continuity of the y-coordinate of footpoints does not guarantee the continuity of the total footpoint displacement (Low & Wolfson 1988). In this study, we employ a continuous shear profile antisymmetric with respect to the $x = 0$ axis and avoid a discontinuity of the total footpoint displacement.

Our numerical equilibrium solutions are performed in a two-dimensional (x, z) computational domain in terms of a rectangular (x, y, z) coordinate system. A rigid boundary is assumed on the $z = 0$ plane where no flow is allowed to move across, which is reasonable considering that the density in the photosphere is far higher than in the corona. Due to this setup, the total mass per flux tube, $M(A)$, in the domain above the rigid boundary is conserved. In constructing equilibria solutions, the invariance of the field line topology is also imposed as a constraint.

3. CURRENT SHEET FORMATION BY THERMODYNAMIC CHANGE

To study the effect of thermodynamic property change on current sheet formation, we will ignore the effect of the toroidal magnetic field and consider a uniform temperature. The above analytical two-dimensional MHS equilibrium solutions without null-points in the magnetic field configurations (Low 1992), equations (18)–(20), are adopted as initial configurations to calculate the total mass density per unit flux tube for our numerical study. As a boundary condition in the $z = 0$ plane, the magnetic flux value, $A(x, z = 0)$, is fixed as the plasma temperature is changed so that the magnetic field footpoints are rooted rigidly at the $z = 0$ boundary. To obtain equilibrium solutions, instead of solving the Grad-Shafranov equation directly, we shall employ a magneto-frictional method (Chodura & Schlüter 1981) to integrate the MHD equations, equations (1)–(7). Faraday's law and Ohm's law without plasma resistivity can be combined in the two-dimensional limit to give

$$\frac{\partial A}{\partial t} = -\boldsymbol{v} \cdot \nabla A\,. \tag{29}$$

When the numerical solutions reach a steady state with terms containing the fluid velocity being asymptotically small in comparison with other terms, they essentially satisfy the Grad-Shafranov equation. For different values of plasma temperature, the new plasma equilibrium pressure distribution will be very different from the simple quadratic form used to obtain $M(A)$. Note that the new equilibrium configuration must have the same magnetic field topology as the analytical solutions because of the plasma frozen-in condition.

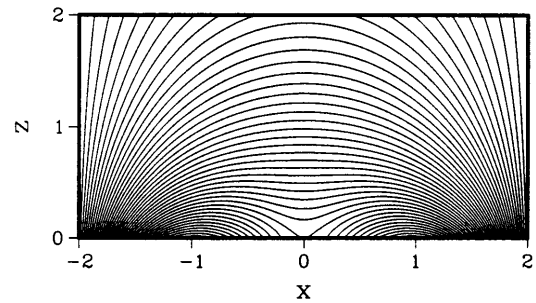

FIG. 2.—Potential field configuration for determining the mass per flux $M(A)$, with $T = 1.0T_0$.

3.1. *Atmospheric Heating*

In the increasing temperature case, we obtain mass per flux tube, $M(A)$, from a simple quadrupolar potential field solution $[a = 0$ so that $\hat{p}(A) = \hat{p}_0]$ with $a_3 = 0.31$, $k = \pi/2L_x$, $L_x = 2$. The potential field configuration is shown in Figure 2. For this case $M(A)$ is larger in the inner flux tube than the outer ones as shown in Figure 3. The scale height is chosen to be a constant and is normalized to $H = 1$. The corresponding mass density is a function of height alone and the mass per flux is maximum at the center of the low-lying bipolar arcades. Note that A^2 is maximum at the center of the low-lying arcades.

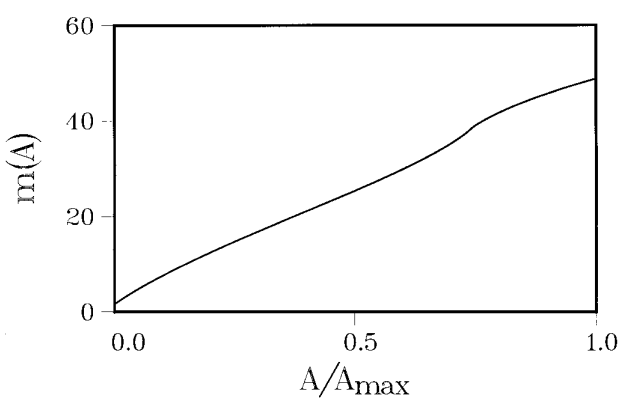

FIG. 3.—Mass per flux $M(A)$ as a function of A for the heating case

As the plasma temperature is uniformly increased, a pressure gradient is developed so that the combined pressure gradient and gravitational force is in the direction pointing away from the center of each arcade and the magnetic field lines expand outward to confine the plasma. Figure 4 shows a sequence of the magnetic field line structure, $J_y(x, z)$ and $\rho(x, z)$ as the plasma temperature is increased from the initial temperature T_0 to $5T_0$. Because of

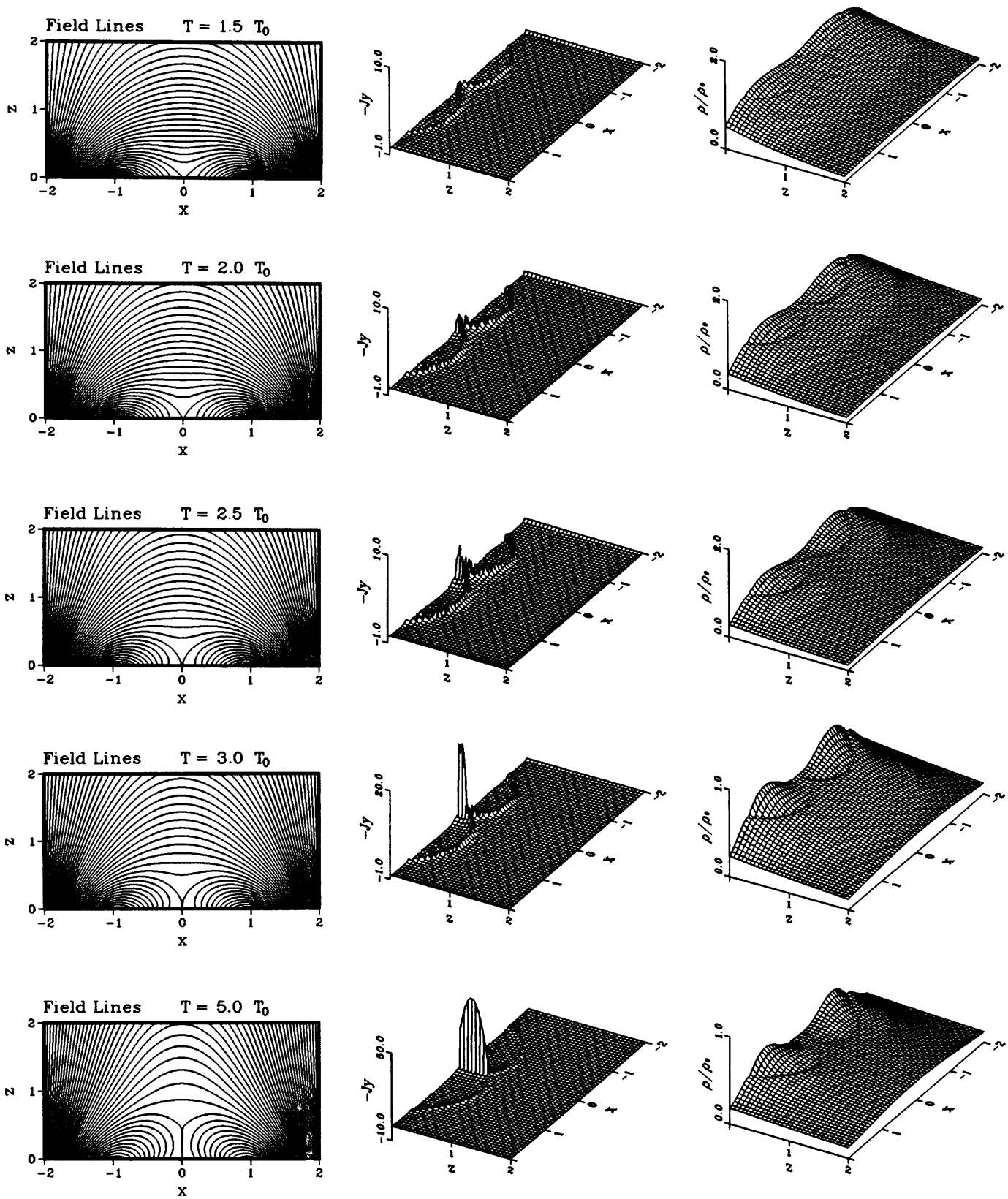

FIG. 4.—Current sheet formation by atmospheric heating. Magnetic field line structure and current density $J_y(x, z)$ are shown for different plasma temperatures.

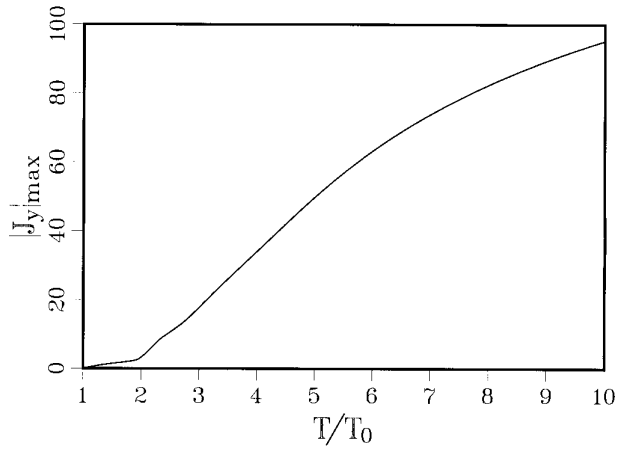

FIG. 5.—Maximum current density $J_y(x, z)$ vs. temperature for the heating case. There is a transition in temperature dependence near $T = 2T_0$, above which the maximum current density increases faster with increasing T.

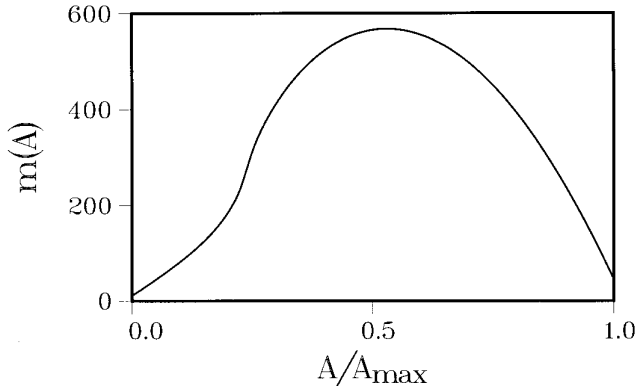

FIG. 7.—Mass per flux $M(A)$ as a function of A for the cooling case

the conservation of mass per flux tube $[M(A)]$ the resulting $\hat{p}(A)$ increases more in the inner flux tubes than in the outer ones as the temperature increases. Because the plasma expansion is more effective in the outer flux tubes than in the inner ones, the combined pressure gradient and gravitational force pushes out the field lines in each bipolar region so that a current sheet of a finite length is formed where the field lines from each bipolar region come into contact. As the temperature increases above a critical value T_c (for this case $T_c \simeq 2T_0$), a current sheet stars to form near the ($x = 0$, $z = 0$) location. The current sheet in this case grows in height from the bottom boundary and extends upward along the whole separatrix $J_y = (d\hat{p}/dA)e^{-z/H}$ and the plasma density has the same spatial variation as the plasma pressure, the thin current sheet should correspond to a sharp local density gradient as shown in Figure 4. With the ideal MHD constraint, the J_y in the current sheet should be infinite. But, numerical calculation provides a finite value due to numerical diffusion. From the dependence of the maximum current density versus the plasma temperature as shown in Figure 5, there is a transition in temperature dependence near $T = 2T_0$, above which the maximum current density increases faster with increasing T. This transitional temperature is interpreted as the critical temperature for the current sheet formation. Note that the magnetic field lines at the current sheet forms a cusplike shape.

3.2. *Atmospheric Cooling*

In the case of decreasing temperature, to constrain the mass per unit flux we choose a smooth equilibrium solution (Low 1992) with $a = -1.5/(2\pi)^2 < 0$, $a_3 = 0.69$, $k = \pi/2L_x$, $L_x = 2$, $s = 2kH = 0.5$, $q^2 = 8aH^2$. Figure 6 shows the magnetic field configuration and corresponding $J_y(x, z)$ and $\rho(x, z)$. The scale height is chosen to be a constant and is normalized to $H = 1$. For this choice, $\hat{p}(A)$ is higher in the outer tubes than in the inner ones so that the combined pressure gradient and gravitational force pushes down the field lines toward the center of each bipolar region. For this choice, $M(A)$ increases with A for $A < 0.55A_{max}$ and then decreases with A for $0.55 < A < A_{max}$ as shown in Figure 7. While the potential field subject to the same boundary condition has an X-point, this initial equilibrium field has none because the combined pressure gradient and gravitational forces depresses the field lines downward.

Figure 8 shows the equilibrium sequence of the magnetic field line structure, $J_y(x, z)$ and $\rho(x, z)$ as the plasma temperature is decreased from the initial temperature T_0 to $0.1T_0$. As the whole atmosphere is uniformly cooled down, the combined pressure gradient and gravitational force is reduced. The magnetic tension force then expands the field lines outward. As the temperature is decreased below a critical value, the subsequent expansion of field lines creates a current sheet (tangential discontinuity). The critical temperature is about $0.25T_0$. The topology of the current sheet in this case is different from that in the former heating case in that a sharp-pointed end of the current sheet hangs a distance above the bottom boundary. As will be shown in

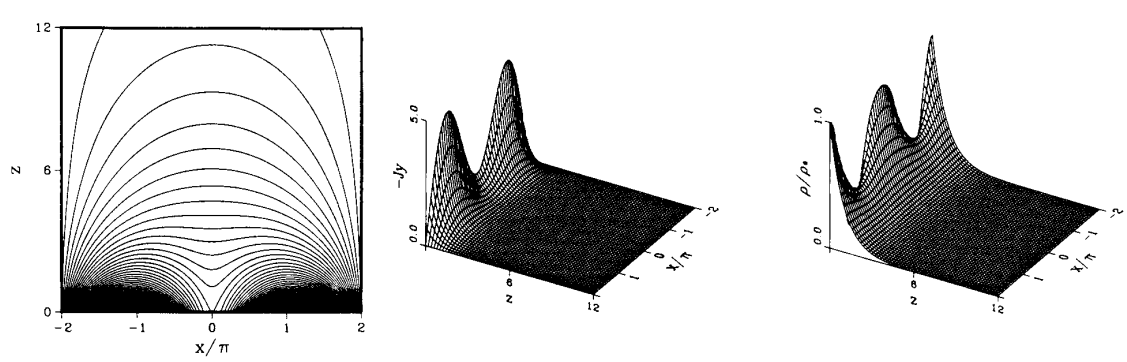

FIG. 6.—Magnetic field configuration and corresponding $J_y(x, z)$ and $\rho(x, z)$ for determining the mass per flux $M(A)$, with $T = 1.00T_0$

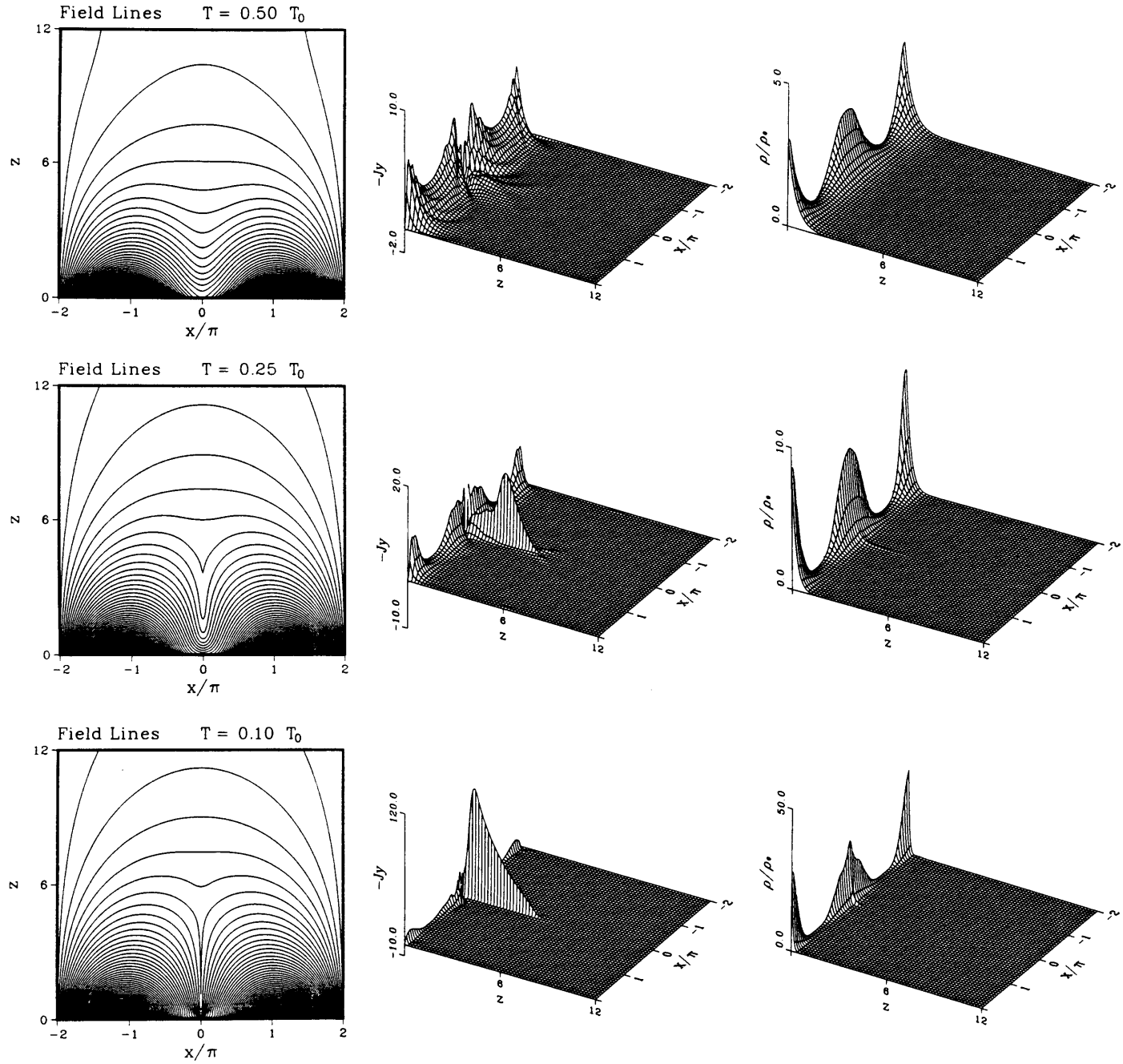

FIG. 8.—Current sheet formation by atmospheric cooling. Magnetic field configuration and corresponding $J_y(x, z)$ profiles are shown for different temperatures.

§ 5, when resistive reconnection processes is simulated, this weak equilibrium state evolves into a Malville-type field configuration embracing a magnetic island. It is expected that a prominence can stably reside within the magnetic island.

4. CURRENT SHEET FORMATION BY FIELD LINE FOOTPOINT MOTION

Low (1987) first showed an explicit example of current sheet formation by continuous footpoint displacements. In his example, a converging footpoint motion pushes the two inner bipolar arcades in a quadrupolar field toward each other so that a current sheet is formed between them. By the same token, Low & Wolfson (1988) argued that a footpoint shearing motion can also expand each arcade to form a current sheet between them. However, the argument in the footpoint shearing case gave rise to controversies. In a simulation study, Karpen, Antiochus, & DeVore (1990) allowed magnetic flux to move freely across the bottom boundary and found that the field line, which originally touched the origin, was levitated by the footpoint shearing motion. They concluded that the current sheet formation proposedby Low & Wolfson (1988) is unphysical because it requires an infinite mass to pin down the field line at the origin. Refuting this criticism, Low (1991) argued that it is impossible for all the field lines to rise above the photo-

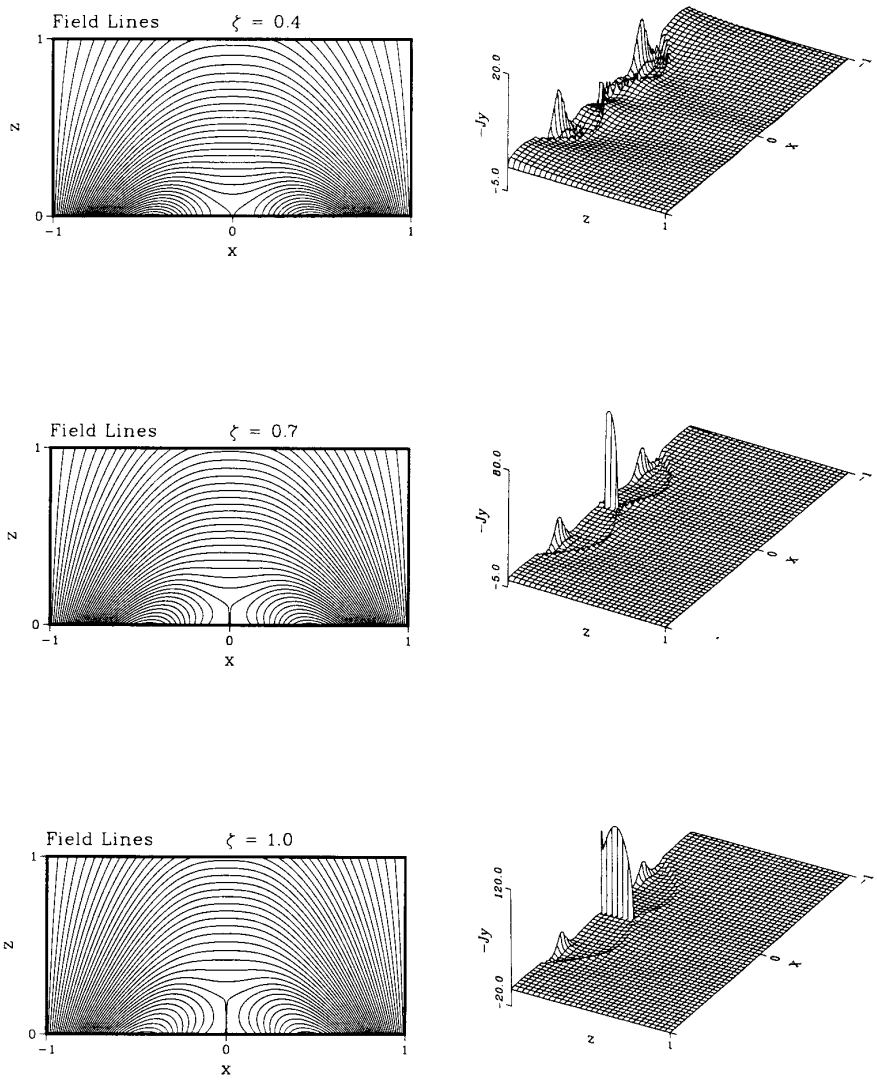

FIG. 9.—Formation of a current sheet by footpoint displacement. A sequence of equilibrium magnetic field configurations and corresponding $J_y(x, z)$ distributions for three different footpoint displacement values are shown. It is to be noted that the current sheet extends along the separatrix field lines.

sphere because of the high mass density in and below the photosphere. He also suggested a possible current sheet configuration with a lower tip curved around by dipped field lines. Our field configuration shown in Figure 8 explicitly demonstrates the existence of such a current sheet and can bring an end to this debate.

In a complex field topology, the footpoint displacement may not be continuous even though the shearing velocity profile is continuous. An example of such a case can be found in a quadrupolar field topology when a footpoint shearing motion is applied to only one side of the lower and upper flux systems (Low & Wolfson 1988). The current sheet formation in this case is so obvious that it does not need to be tested by numerical simulation. Instead, we will consider cases with both the shearing velocity profile and the resulting footpoint displacement being everywhere continuous. Specifically we shall impose a spatially continuous footpoint shearing motion with the velocity profile $V_y(x, z = 0) = V_{y0} \sin [\pi(x - X_0)/(1 - X_0)]$ for $1 \geq x \geq X_0$ and $V_y(x, z = 0)$ for $X_0 > x \geq 0$, where X_0 is the position of the low-lying arcade center. The shearing velocity profile is antisymmetric with respect to $x = 0$ to exclude pathologic cases in which the toroidal field has a discontinuity for any nonzero amount of shear. The maximum shearing velocity is $V_{y0} = 0.0025 V_A$, where V_A is the Alfvén speed at $x = 1$, $z = 0$. A quadrupolar potential field in a low β ($\beta = 0.005$ at $x = 1$, $z = 0$) plasma is considered as the initial equilibrium configuration. We shall also assume the constraint of the conservation of total mass per flux tube. However, because the plasma β is small, the mass conservation constraint and the gravity have smaller effects on the equilibrium structure than the field line footpoint motion for typical active time parameters. To follow the quasi-static evolution of the magnetic field configuration, a time-dependent ideal MHD simulation based on equations (1)–(7) is performed. The maximum shearing velocity is chosen to be much smaller than the Alvén velocity so that the plasma will be in quasi-static equilibrium states.

As the shear increases, the field line displacement (and thus the toroidal magnetic field B_y) increases, and the gradient force of the toroidal magnetic field pressure pushes the field lines of low-lying bipolar arcades outward and expels the field lines belonging to the upper arcade from between them. Above a critical amount of footpoint displacement,

the field lines in the bipolar arcades come into contact to form a tangential discontinuity (current sheet) between those two arcades. Figure 9 shows a sequence of equilibrium magnetic field configurations and corresponding $J_y(x, z)$ distributions for three different footpoint displacement values. The critical maximum footpoint displacement is just above $\zeta = 0.4$. The current sheet configuration is same as that shown in Figure 4 for the temperature case. Our result may be an example of current sheet formation by general footpoint displacements previously suggested by Parker (1972). If resistivity is applied to this current sheet configuration, magnetic reconnection changes the field topology into one with an X-point.

5. FORMATION OF SOLAR PROMINENCE

Solar prominences are remarkable structures of cool (5000 to 8000 K) and dense (10^{11} cm^{-3}) material, suspended in the hot (10^6 K) and tenuous (10^8 to 10^9 cm^{-3}) solar corona. Prominences are mostly located above the magnetic neutral lines, and this suggests the support of prominence material by magnetic fields. The prototype static models by Kippenhahn & Schlüter (1957) and Kuperus & Raadu (1974) represent two different field topologies or polarities of prominences. In normal-polarity prominences represented by the Kippenhahn-Schlüter model, the direction of the magnetic field normal to the prominence plane is parallel to that of the plausible ambient field, while it is reversed in inverse polarity prominences represented by the Kuperus-Raadu model. According to coronagraph observations (Leroy 1989), there are 3 times as many inverse polarity prominences as normal polarity prominences. A statistical study by Tang (1987) showed that more prominences are formed beween bipolar regions than inside a bipolar region. This result is far from surprising because current sheet formation seems quite common between two bipolar regions as discussed in the previous sections. As a result of magnetic reconnection processes the current sheets can evolve into field configurations favorable to supporting prominence material.

We have investigated what effect resistivity can bring about in a current sheet. Imposing resistivity to a current sheet, we have found that the global field evolution during the reconnection process depends on the size of the diffusion region. A fast magnetic reconnection with a small shock angle can be achieved only with a locally enhanced resistivity pattern.

A self-contained model of a solar prominence between two bipolar regions was given by Choe (1995). If the bottom of the current sheet touches the photosphere as in the heating and footpoint shearing cases, resistive reconnection leads to a configuration with an X-point. The upward transport of plasma from the X-point enhances the density in the overlying arcade where a thermal instability sets in. The successive condensation leads to the formation of an inverse polarity prominence where the cold and dense plasma can sit on the field lines above the X-point. In Figure 10 the upper figures show the current sheet configuration and current density $J_y(x, z)$ for the footpoint shearing case with $\zeta = 2.0$. The lower figures show the resultant prominence field configuration and current density $J_y(x, z)$ for a magnetic Reynold's number of 10^4. In this case, an inverse polarity prominence is expected above an X-point without a magnetic island. This prominence field configuration is quite different from the conventional prominence field configurations in a bipolar field geometry: the Kippenhahn-Schlüter type field configuration that is related to the normal polarity condition and the Kuperus-Raadu type field configuration that is related to the inverse polarity condition.

In a discussion reported by Anzer (1979), Malville suggested another field geometry such as that shown in Figure 11 as a plausible model of prominence magnetic fields. In this model, a magnetic island is wrapped by Kippenhahn-Schlüter type field lines. Hirayama (1985) speculated that as

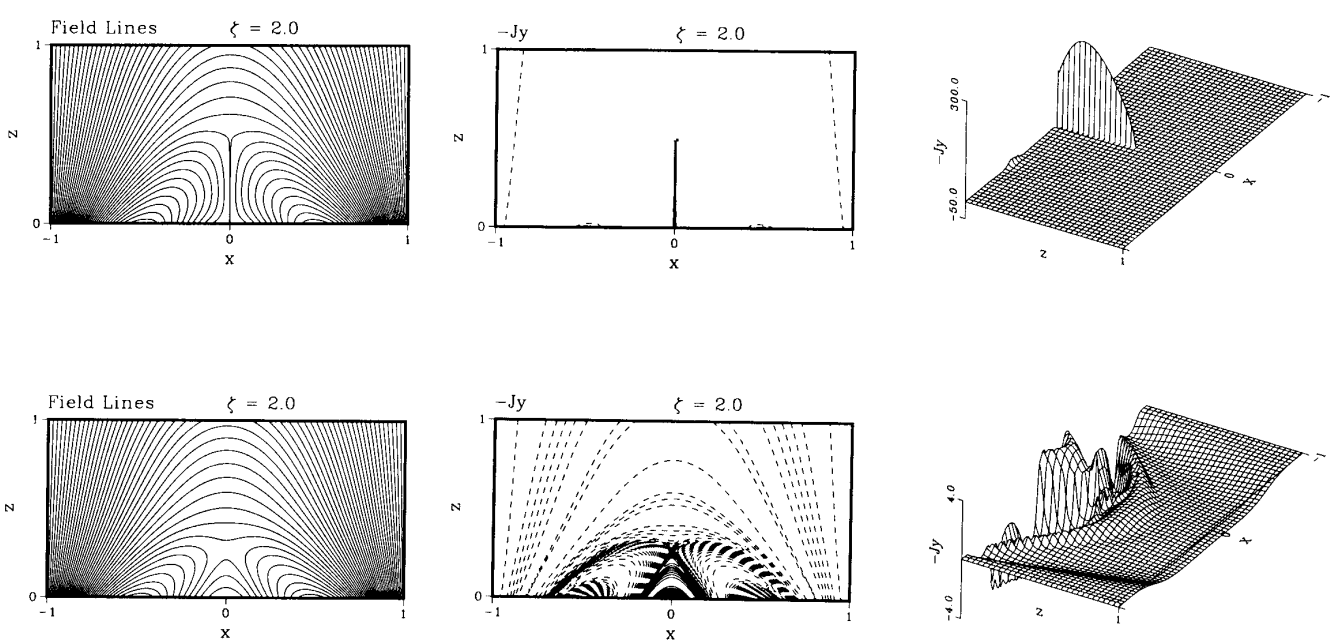

FIG. 10.—Upper figures show the current sheet configuration and current density $J_y(x, z)$ with a maximum shearing displacement $\zeta = 2.0$, and the lower figures show the resultant prominence field configuration and current density $J_y(x, z)$ for a magnetic Reynold's number of 10^4.

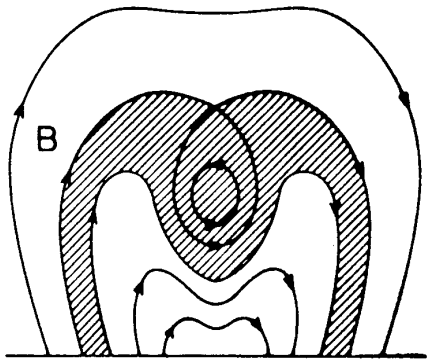

FIG. 11.—Prominence field model suggested by Malville (Anzer 1979). The shaded area indicates the location of the prominence material.

the prominence mass becomes larger, the field lines of a Kippenhahn-Schlüter type prominence sag more and more, and the top of the dipped field lines can finally be reconnected to form a magnetic island. However, a simulation study by Choe & Lee (1992) showed that the dip does not become significantly deep even after the prominence mass becomes very large. Furthermore, that mechanism is unlikely to work in a very low β plasma.

We have investigated the formation of Malville's model of prominence field configuration. Starting with the current sheet equilibrium with $T = 0.25T_0$ as shown in Figure 8, we performed a resistive MHD simulation with a uniform resistivity (magnetic Reynold's number $= 10^4$) by slowly lowering the temperature. Magnetic reconnection takes place in the current sheet and a vertically elongated magnetic island is formed in a thin current layer as shown in Figure 12 which shows the field configuration and $J_y(x, z)$ for two cases with $T/T_0 = 0.16$ and 0.13, respectively. The density in the island is higher than that in the surrounding region which is clearly seen in the enlarged pictures of field configuration, $J_y(x, z)$ and $\rho(x, z)$ for $T = 0.13T_0$ as shown in Figure 13. This prominence model of plasma and magnetic field configurations is of an inverse polarity type. Although the results were obtained using a two-dimensional isother-

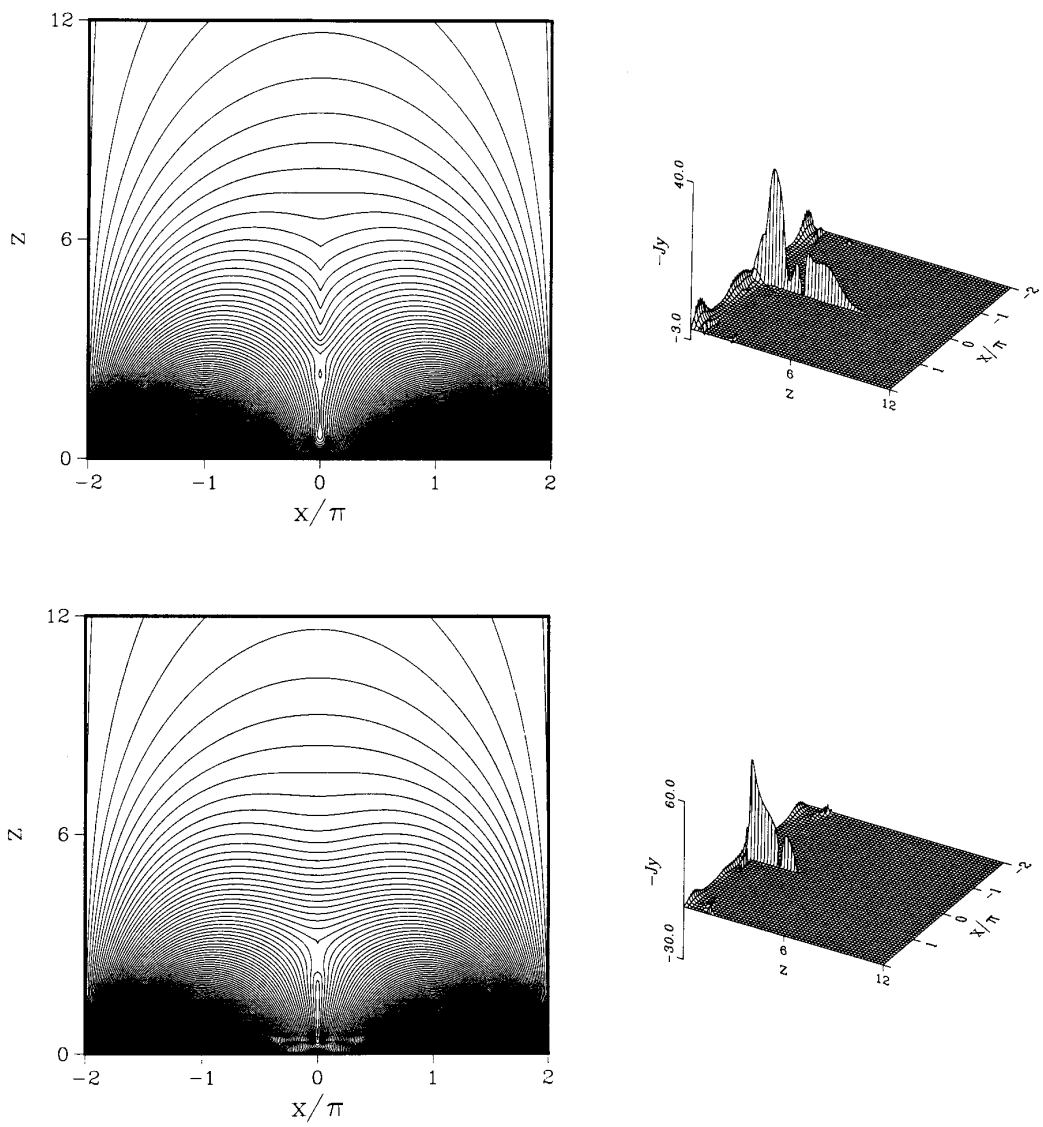

FIG. 12.—Field configuration of a vertically elongated magnetic island formed in a thin current layer and corresponding $J_y(x, z)$ for two cases with $T/T_0 = 0.16$ and 0.13, respectively.

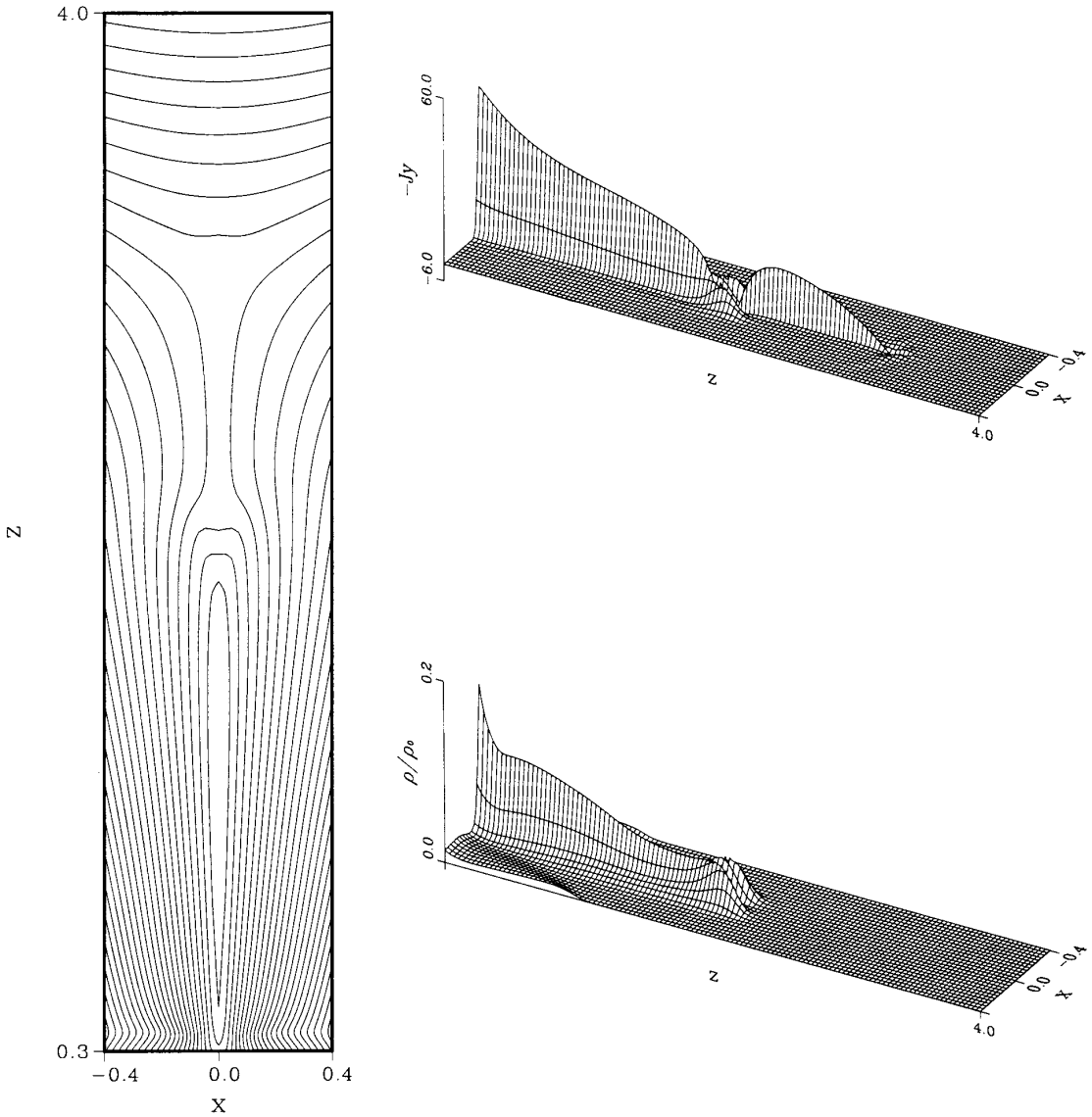

FIG. 13.—Enlarged pictures of field configuration, $J_y(x, z)$ and $\rho(x, z)$ for $T = 0.13T_0$

mal model, it shows for the first time how a magnetic island can be formed between two bipolar regions.

6. SUMMARY AND DISCUSSION

In this paper we have obtained weak equilibria containing current sheets in a two-dimensional quadrupolar magnetic field geometry by pressure gradient force effects as well as by the conventional field line footpoint displacement. We have shown that a magnetohydrostatic equilibrium without null points can be deformed into an equilibrium field configuration containing current sheets (tangential discontinuities) either by changes in thermodynamic properties or by footpoint displacement or a combination of these effects. From the results we suggest that the current sheet formation must be quite ubiquitous in the solar atmosphere. We have also shown that via resistive magnetic reconnection processes the current sheets can evolve into field configurations supporting inverse polarity type prominence material.

The shape of current sheets depends on the pressure distribution in flux tubes and can be understood based on the force balance consideration. Under a constant gravitational force pointing downward in the negative z-direction, the pressure can be written as $\hat{p}(A)e^{-z/H}$, where A is the magnetic flux function and H is the pressure scale height. The combined pressure gradient and gravity force is given by $-\nabla\hat{p}(A)e^{-z/H}$. If $\hat{p}(A)$ is higher in the lower flux tube than the higher ones in each bipolar arcade, the combined pressure gradient and gravitational force pushes magnetic field lines outward from the center of each bipolar arcade. If the plasma temperature is increased above a critical value, the enhanced expansion of these field lines results in the formation of a current sheet between these two arcades along a separatrix line. Similarly, when the field line footpoints undergo a spatially continuous shearing motion, a sheared magnetic field is generated. For a footpoint displacement profile producing an outward gradient force of the sheared magnetic field pressure which pushes the field lines of each

bipolar arcade into contact, a current sheet of the same shape can be found if the amount of shear is above a critical value. This field configuration can be deformed into a configuration with an X-point through resistive magnetic reconnection. It is expected that an inverse polarity prominence can stably reside above the X-point.

If $\hat{p}(A)$ is higher in the outer rather than inner tubes of the bipolar arcades, the combined pressure gradient and gravitational force which pushes down magnetic field lines is reduced when the atmosphere is cooled. When the temperature is decreased below a critical value, the subsequent expansion of field lines due to the magnetic tension force creates a new current sheet configuration with a sharp downward-pointed tip hanging at a distance above the bottom boundary. Resistive magnetic reconnection in this type of current sheet results in a Malville-type field configuration with a magnetic island wrapped in dipped field lines. It is expected that an inverse polarity prominence can stably reside within the magnetic island.

Although our model is based on a two-dimensional geometry, we may find a realization in the real Sun by the aid of observation. Heating and radiation cooling of corona and field line footpoint motion are on-going processes in the solar atmosphere. Thus, we have to look for a signature of the subsequent magnetic reconnection between two bipolar arcades. The prominence field configuration with a magnetic island located in a field line dip has long been speculated as a possible field geometry of normal polarity prominences. The original Kippenhahn-Schlüter type field configuration does not seem to hold the prominence material stably against any lateral perturbations. The validity of our model can be determined from measurement of magnetic fields at the top and bottom of a prominence.

To more realistically study the prominence formation, we need to construct three-dimensional current sheet equilibria and consider a combination of all possible physical effects of current sheet formation discussed in this paper. The equilibrium code developed by Chen (1995) can be extended for the solar magnetic field geometry. The construction of a three-dimensional prominence structure in bipolar and quadrupolar geometries will be the next step. The stability of such a structure needs to be studied in conjunction with prominence eruption.

This work was supported by the NSF grant ATM 96-96232 and DoE contract DE-AC02-76-CHO3073. G. S. C. was also partly supported by the Korea Research Foundation. The authors would like to thank B. C. Low for very helpful comments.

REFERENCES

Aly, J. J. 1994, in Cosmical Magnetism, Contributed Papers of the NATO Advanced Research Workshop, ed. D. Lynden-Bell (Cambridge: Inst. Astron.), 7
Aly, J. J., & Amari, T. 1989, A&A, 221, 287
Anzer, U. 1979, in IAU Colloq. 44, Physics of Solar Prominences, ed. E. Jensen, P. Maltby, & F. Q. Orrall (Blindern-Oslo: Inst. Theoretical Astrophys), 322
Cheng, C. Z. 1995, Geophys. Res. Lett., 22, 2401
Cheng, C. Z., & Choe, G. S. 1997, in IAU Colloq. 167, New Perspectives on Solar Prominences, ed. D. F. Webb (Dordrecht: Reidel)
Chodura, R., & Schlüter, A. 1981, J. Comput. Phys., 41, 68
Choe, G. S. 1995, Ph.D. thesis, University of Alaska–Fairbanks
Choe, G. S., & Lee, L. C. 1992, Sol. Phys., 138, 291
———. 1996a, ApJ, 472, 360
———. 1996b, ApJ, 472, 372
Dungey, J. W. 1953, MNRAS, 113, 180
Hirayama, T. 1985, Sol. Phys., 100, 415
Karpen, J. T., Antiochus, S. K., & DeVore, C. R. 1990, ApJ, 356, L67
Kippenhahn, R., & Schlüter, A. 1957, Z. Astrophys. 43, 36
Kuperus, M., & Raadu, M. A. 1974, A&A, 315, 185
Lau, Y. T., & Finn, J. M. 1990, ApJ, 350, 672
Lepeltier, T., & Aly, J. J. 1996, A&A, 306, 645
Leroy, J. L. 1989, in Dynamics and Structure of Quiescent Solar Prominences, ed. E. R. Priest (Dordrecht: Kluwer), 77
Low, B. C. 1987, ApJ, 323, 358
———. 1991, ApJ, 381, 295
———. 1992, A&A, 253, 311
Low, B. C., & Wolfson, R. 1988, ApJ, 324, 574
Martin, S. F. 1973, Sol. Phys., 31, 3
———. 1990, in IAU Colloq. 117, Dynamics of Quiescent Prominences, Lecture Notes in Physics, 363, ed. V. Ruždjak & E. Tandberg-Hanssen (Berlin: Springer Verlag), 1
Mikić, Z., & Linker, J. A. 1994, ApJ, 430, 898
Parker, E. N. 1972, ApJ, 174, 499
———. 1994, Spontaneous Current Sheets in Magnetic Fields (Oxford: Oxford Univ. Press)
Syrovatskii, S. I. 1981, ARA&A, 19, 163
Tang, F. 1987, Sol. Phys., 107, 233
Uchida, Y., Fujisaki, K., Morita, S., Torii, M., Hirose, S., & Cable, S. 1997a, PASJ, submitted
Uchida, Y., Hirose, S., Cable, S., Uemura, S. Fujisaki, K., Torii, M., & Morita, S. 1997b, in IAU Colloq. 167, New Perspectives on Solar Prominences, ed. D. F. Webb (Dordrecht: Reidel)
van Ballegooijen, A. A. 1985, ApJ, 298, 421
———. 1988, Geophys. Astrophys. Fluid Dyn., 41, 181
Zweibel, E. G., & Hundhausen, A. J. 1982, Sol. Phys., 76, 261